New Journal of Physics
The open access journal for physics

Raman study of the Verwey transition in magnetite thin films

M Baghaie Yazdi[1,4], K-Y Choi[2,3], D Wulferding[2], P Lemmens[2] and L Alff[1]

[1] Institute of Materials Science, Technische Universität Darmstadt, Petersenstrasse 23, D-64287 Darmstadt, Germany
[2] Institute for Condensed Matter Physics, Technische Universität Braunschweig, D-38106 Braunschweig, Germany
[3] Department of Physics, Chung-Ang University, 221 Huksuk-Dong, Dongjak-Gu, Seoul 156-756, Republic of Korea
E-mail: mehrdad@oxide.tu-darmstadt.de

New Journal of Physics **15** (2013) 103032 (8pp)
Received 21 August 2013
Published 30 October 2013
Online at http://www.njp.org/
doi:10.1088/1367-2630/15/10/103032

Abstract. We have grown epitaxial thin films of magnetite on MgO and Al_2O_3 substrates with sharp and distinct signatures of the Verwey transition in resistivity and magnetization. We have used Raman scattering to separate the footprint of purely structural changes from the effect of additional charge and orbital order. Raman modes related to the structural phase transition occur first at temperatures above the Verwey transition temperature. In contrast, newly emerging modes indicating additional charge and orbital order appear at the Verwey transition. These results suggest that the completion of the structural phase transition in magnetite is a necessary precursor triggering a transition into a complex charge and orbitally ordered state.

[4] Author to whom any correspondence should be addressed.

Contents

1. Introduction

For decades the metal–insulator transition in magnetite (Fe_3O_4) has been the subject of scientific debate and controversy. Since its discovery by Verwey in 1939 [1] a vast amount of theoretical and experimental work has resulted in the development of various models trying to explain the physical origin of this complex phase transition. Nevertheless, the case is not settled and several questions regarding the nature of the Verwey transition remain unanswered to this day. A recent series of publications based on local density approximation plus Hubbard U band structure calculations suggests the existence of charge and orbital order in Fe_3O_4 below the Verwey transition temperature, T_V [2–4]. The on-site correlations of the 3d electrons play the key role for charge–orbital ordering, while the structural distortion is necessary to obtain the empirically observed insulating gap [4]. Experimentally, a Bragg forbidden peak at $(00\frac{1}{2})_c$ (the subscript c refers to the high-temperature cubic unit cell) observed by resonant soft x-ray diffraction (RSXD) on Fe_3O_4 thin films ($T_V = 115$ K) occurs only in the Verwey state and has been interpreted as a direct measure of t_{2g} orbital order at the octahedral Fe^{2+} sites [5]. From this, it has been concluded that orbital order is the driving force of the Verwey transition [6]. It has also been argued that charge and orbital order occur at a characteristic temperature 10 K above the Verwey transition which itself is, then, a reaction of the lattice to the charge disproportionation [7]. In opposition to the above interpretation, it has been claimed that the observation of the forbidden $(00\frac{1}{2})_c$ Bragg peak can also be accounted for in terms of merely structural displacements [8]. The corresponding measurements were performed on single crystals with $T_V = 120.6$ K (from specific heat). The current discussion results in the key question whether the driving force behind the Verwey transition is of structural or charge/orbital origin [9, 10]. It is obvious that lattice, electronic and magnetic degrees of freedom are strongly coupled in magnetite and display a delicate interplay [11–13]. In order to disentangle the different contributions to the Verwey transition, we have revisited this problem using Raman spectroscopy in high-quality thin films of magnetite showing more pronounced features in the Raman spectra as compared to available single crystal data.

Raman spectroscopy has not only the advantage of being bulk sensitive as compared to soft x-ray methods but also has been successfully applied to systems with orbital order [14, 15]. We followed the suggestion of Honig [17] to use only samples for our studies which show a Verwey transition around or above 120 K, since it is well-known that the Verwey temperature is the most sensitive measure of disorder. Even more, we have used only optimized thin films showing both, a sharp transition in magnetization as well as in transport data.

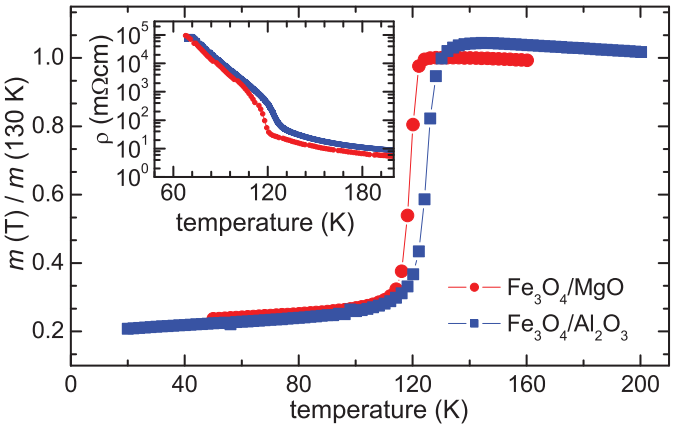

Figure 1. Temperature dependence of the magnetization of Fe_3O_4 thin films on MgO (light (red) symbols) and Al_2O_3 (dark (blue) symbols). The inset shows resistivity versus temperature.

2. Experimental

Raman scattering experiments were performed in quasi backscattering geometry using an Ar–Kr ion laser at $\lambda = 488$ nm with a laser power of 10 mW and a spot diameter of 100 μm to avoid sample overheating [18]. The samples were installed in a He-cooled closed cycle cryostat with a temperature range of 3–300 K. The spectra were collected via a Dilor-XY 500 triple spectrometer by a liquid nitrogen cooled HORIBA Jobin Yvon CCD (Spectrum One CCD-3000 V). The background of the measured Raman spectra have all been Bose corrected.

3. Results and discussion

We have chosen two samples sputtered on c-Al_2O_3 and MgO with extremely pronounced Verwey transitions in both, resistivity and magnetization, and clearly distinct T_V in order to be able to track the changes of Raman modes through T_V. In figure 1 the magnetic and electronic properties of both films are shown. The magnetization was measured in an external field of $H = 500$ Oe while heating through the Verwey transition after zero field cooling. The film on Al_2O_3 shows a higher phase transition temperature compared to the film on MgO. In order to further quantify the Verwey transition of our samples, we have determined three parameters from the second derivative of the temperature dependence of magnetization and resistivity. The onset temperature, T_{onset}, of the transition is defined by the associated peak in the second derivative of the corresponding quantity. The Verwey transition itself is defined as the midpoint of the transition (peak in the first derivative as commonly defined in literature). The temperature of the endpoint of transition is again obtained from the associated peak in the second derivative. The difference in onset and endpoint temperature defines the transition width ΔT. It is remarkable that the Fe_3O_4 film on Al_2O_3 has a Verwey transition at $T_V^m = 128$ K ($\Delta T = 12$ K) as compared to $T_V^m = 119$ K ($\Delta T = 10$ K) for the film on MgO. The index m indicates that these values refer to the magnetization measurements. From the viewpoint of resistivity (index r), $T_V^r = 123$ K for the film on Al_2O_3, and $T_V^r = 118$ K for the film on MgO. Typically, films on MgO show higher crystallinity [16] but reduced transition temperature.

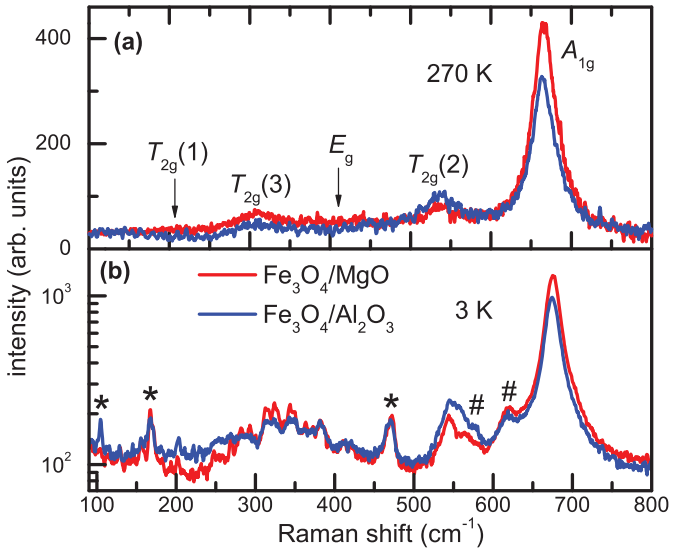

Figure 2. Raman spectra of Fe_3O_4 on MgO (light (red) line) and on Al_2O_3 (dark (blue) line) measured (a) above T_V at $T = 270\,K$ and (b) below T_V at $T = 3\,K$. The asterisks mark newly activated modes induced by the Verwey transition. The hashs mark evolving shoulder modes to the main modes.

Since the observation of a metal–insulator transition in the resistivity requires a global phase transition in the sample, it is expected that $T_V^r \lesssim T_V^m$.

Figure 2 shows the Raman spectra of both films measured above ($T = 270\,K$) and below ($T = 3\,K$) the Verwey transition. In the high-temperature phase we see three main modes: A_{1g} at $665\,cm^{-1}$, $T_{2g}(2)$ at $538\,cm^{-1}$ and $T_{2g}(3)$ at $310\,cm^{-1}$. Both, the E_g and the $T_{2g}(1)$, mode are barely visible at 380 and $205\,cm^{-1}$, respectively (see the arrows in figure 2(a)). The spectra qualitatively agree well with previously reported Raman data on single crystals and thin films [18, 19, 20–22]. Note that the symmetry assignment of the modes is not yet consistent in literature[5]. The $T_{2g}(3)$ mode is weak and broad. It is associated with an asymmetric bending of oxygen with respect to the Fe atoms [23], implying that the mode displacement is highly sensitive to valence fluctuations or dynamic distortions of the FeO_6 octahedra.

In the Verwey phase a large number of new modes and features show up—a hallmark of Raman measurements on magnetite not observed in any other material. Only a few of these modes can be directly attributed to the structural transition into the monoclinic structure having *Cc* space group symmetry below T_V [24]. At room-temperature, all *A*-site tetrahedra are equivalent. The oxygen vibrations of these tetrahedra are responsible for the A_{1g} mode [23], the strongest mode observed in the Raman spectra. As indicated in figure 3, in the monoclinic structure the A-site tetrahedra are symmetrically not equivalent. As the environments are slightly different, one expects a splitting of the main mode. Indeed, one observes shoulder modes evolving from the A_{1g} and $T_{2g}(2)$ modes. These modes are indicated in figure 2(b) by hash symbols. According to the structural model one could expect even the appearance of several shoulder modes. Note, however, that neither the structure itself has been confirmed, nor are any theoretical predictions to be expected soon due to the huge unit cell. Currently, only the simpler monoclinic $P2/c$ unit cell has been theoretically investigated [13]. In contrast, the peaks at

[5] The symmetry assignment of the $T_{2g}(3)$ and E_g modes is sometimes reversed [11].

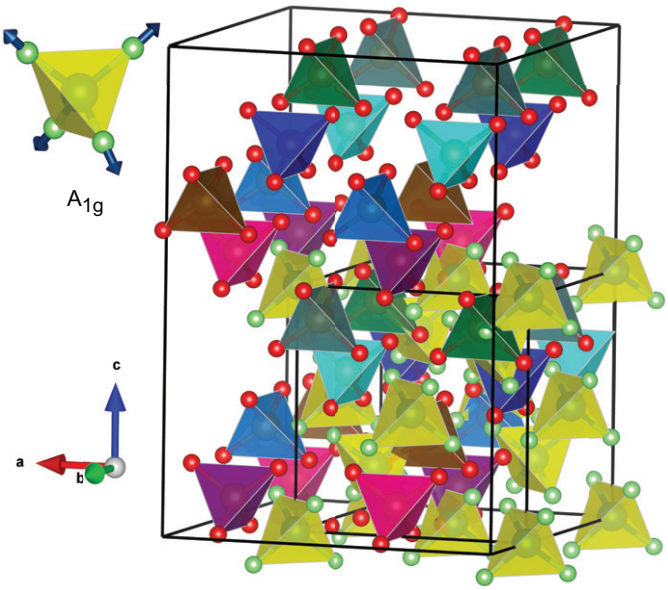

Figure 3. One unit cell of the crystal structure of magnetite in the Verwey phase (*Cc* space group symmetry, no. 9). Highlighted are the oxygen tetrahedra at the iron A-site. In the cubic structure above the Verwey transition (small unit cell), all tetrahedra (drawn in light grey (yellow) are equivalent. In the *Cc* structure the different grey shades (colours) represent non-equivalent tetrahedra (structural data courtesy of Senn *et al* [24]).

104, 171 and 472 cm^{-1} (marked by asterisks in figure 2(b)) are of different origin because they are sharp and have no direct relation to the major modes. Such peak shapes are discussed to be related to charge and orbital order [25–27]. In the suggested charge–orbital ordered phase, off-centre atomic displacements lead to substantial electrical polarization, yielding these newly activated Raman modes. The most distinct change below the Verwey transition is observed in the $T_{2g}(3)$ mode. Below T_V, it consists of a dozen of sharp peaks superimposed on a broad Gaussian background. The line shape of the background and the number of the superstructure induced peaks suggest that a complex orbital and charge order is present which leads to new periodicities. In contrast to the shoulder modes, these new modes can be considered as an indicator of the presence of additional (charge and orbital) order.

Figure 4 shows the temperature dependence of the phonon parameters (frequency, linewidth and normalized intensity) for the major modes of both films. All three modes display an abrupt change in their phonon parameters through the Verwey transition. In the narrow temperature interval around T_V, both the A_{1g} and the $T_{2g}(2)$ mode undergo a strong hardening by 5 cm^{-1} while their linewidths drop drastically and their scattering intensity grows by almost one order of magnitude upon temperature decrease. The $T_{2g}(3)$ mode shows a more drastic change of frequency and intensity. Contrarily to the former modes, the linewidth increases upon cooling through T_V since the line broadening is related to the superstructure. The abrupt large hardening across T_V indicates the effect of the changes in the lattice forces due to charge and orbital order and the related changes in the Coulomb energies. The transition to an insulating state can lead to an enhancement of phonon scattering intensity. However, the observed huge jump involves a strong change of electronic polarizabilities since the scattering intensity relies on the variations of the dielectric function with respect to the normal mode displacement.

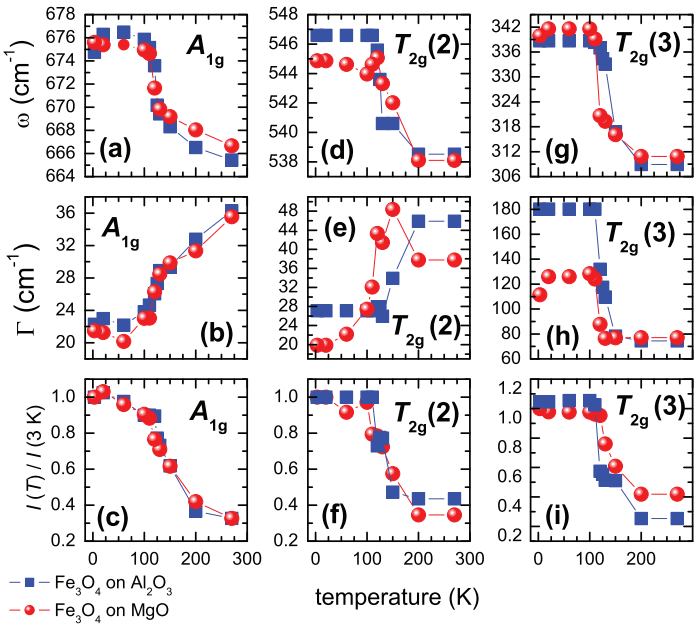

Figure 4. Temperature dependence of the frequency, the linewidth and the normalized intensity for the A_{1g}, the $T_{2g}(2)$ and the $T_{2g}(3)$ phonon modes. Filled (blue) squares are for the film on Al_2O_3, filled (red) circles for the film on MgO. The solid lines are guides to the eyes.

Furthermore, the relative increased hardening with respect to the other modes may also be related to the vicinity of the gap in the electronic band structure reported to be around 40 meV [28, 29]. The anomalous increase in linewidth through T_V is associated with an increased phonon lifetime. Since the material is strongly insulating below T_V, spin–phonon coupling maybe increased below T_V [30]. In general, it seems to be a generic feature of magnetite that phonons are strongly coupled to charge–orbital fluctuations [31].

The most important part of our analysis consists of a quantitative analysis of the temperature evolution of the spectral weight of the different Raman modes shown in figure 5. It allows to differentiate modes with respect to energy and temperature dependence. Modes that appear at the shoulder of room-temperature modes are already clearly visible for $T \approx T_V$. In contrast, modes not related in energy to room-temperature modes start to evolve only at T_V and are clearly observed only at lower temperature, $T \ll T_V$. Using these modes, we contrast the effect of structural symmetry lowering with the effect of charge and orbital order at lower temperature [25–27]. In the upper row of figure 5 we show the experimental spectra at different temperatures above and below the transition. Below each graph the refinement of the spectral weight is shown for both films. For the film on sapphire already at 150 K the first indication of the shoulder modes at the A_{1g} and $T_{2g}(2)$ modes can clearly be distinguished while the same shoulders develop for the film on MgO only at 130 K. Only at 120 K the film on Al_2O_3 shows the formation of new modes including the sharp modes on the $T_{2g}(3)$ mode, and a new sharp mode at 472 cm^{-1}. The evolution of the spectral weight of the shoulder modes is not systematic. Unfortunately, there are no theoretical prediction possible due to the low symmetry of the unit cell. Nevertheless, the evolution of the shoulder modes well above T_V is unambiguous. Note that both films exhibit almost identical types of features in the spectra well below the Verwey

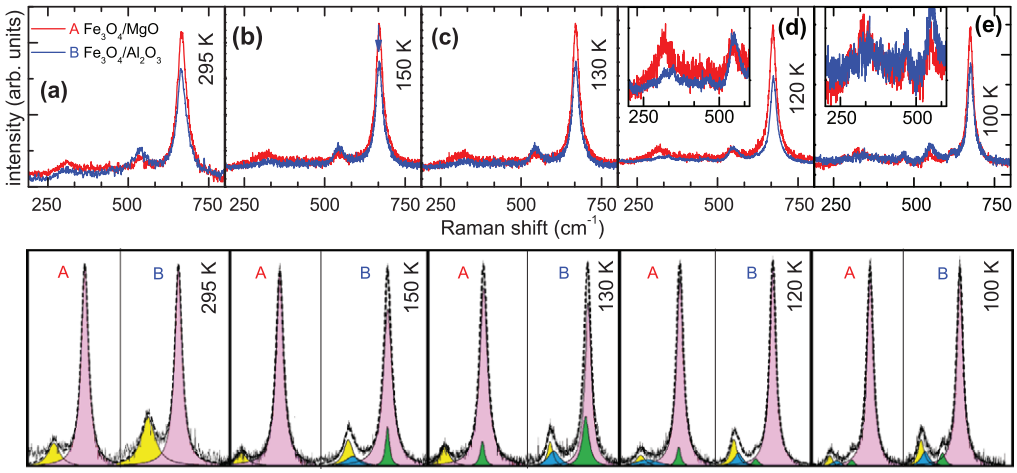

Figure 5. Top row: temperature evolution of the Raman modes measured at (a) 295 K, (b) 150 K, (c) 130 K, (d) 120 K and (e) 100 K. Bottom row: refined modes (intensity is normalized). The spectra are fitted in the range of 480–800 cm^{-1}. Red and yellow indicate the spectral weight of room-temperature modes, green and blue the spectral weight of the emerging shoulder modes.

transition (100 K). This indicates that we observe indeed the intrinsic (sample independent) temperature evolution of the transition into the Verwey state. The shoulder modes follow the gradual structural phase transition already well above the long-range order. Consistent with this observation is a recent report of magnetic fluctuations observed by muon–spin spectroscopy as a precursor for the formation of a charge density wave state below T_V [32]. In contrast to the shoulder modes, the modes attributed to charge and orbital order cannot be traced above the temperature where long-range structural order has been achieved. Thus, the completion of the structural phase transition which itself is a result of the interplay of electronic and structural degrees of freedom [31], is a requirement for the formation of the charge and orbitally ordered state. As stated above, the observed spectra are in agreement with single crystal data both, above and below the Verwey transition. Therefore, the features that have been observed more clearly in the thin films are also relevant to the Verwey transition in bulk magnetite.

4. Summary

Summarizing our results, all reported features occur in both thin films at different temperatures but in the same order indicating that we observe intrinsic signatures associated with the Verwey transition. Since the shoulder modes that appear at the highest temperatures compared to other features are related to structural symmetry lowering, we can conclude that the structural transition is a *precursor* of the Verwey transition. Modes which can be attributed most likely to charge and orbital order occur in both films clearly at lower temperatures as compared to the shoulder modes. The magnetic Verwey transition occurs at about the same temperature where these new phonon modes arise. The picture emerging from this data is that in the presence of strong electronic correlations the structural phase transition in magnetite is a necessary prerequisite for the appearance of a complex orbital and charge order as characteristic for the Verwey state.

Acknowledgments

We thank W Donner, J Kreisel and A F Kemper for fruitful discussions.

References

[1] Verwey E J W 1939 *Nature* **144** 327
[2] Leonov I, Yaresko A N, Antonov V N, Korotin M A and Anisimov V I 2004 *Phys. Rev. Lett.* **93** 146404
[3] Jeng H-T, Guo G Y and Huang D J 2004 *Phys. Rev. Lett.* **93** 156403
[4] Zhou F and Ceder G 2010 *Phys. Rev.* B **81** 205113
[5] Schlappa J *et al* 2008 *Phys. Rev. Lett.* **100** 026406
[6] Tanaka A *et al* 2012 *Phys. Rev. Lett.* **108** 227203
[7] Lorenzo J E, Mazzoli C, Jaouen N, Detlefs C, Mannix D, Grenier S, Joly Y and Marin C 2008 *Phys. Rev. Lett.* **101** 226401
[8] Wilkins S B, Di Matteo S, Beale T A W, Joly Y, Mazzoli C, Hatton P D, Bencok P, Yakhou F and Brabers V A M 2009 *Phys. Rev.* B **79** 201102
[9] Rozenberg G Kh, Pasternak M P, Xu W M, Amiel Y, Hanfland M, Amboage M, Taylor R D and Jeanloz R 2006 *Phys. Rev. Lett.* **96** 045705
[10] Szotek Z, Temmerman W M, Svane A, Petit L, Stocks G M and Winter H 2003 *Phys. Rev.* B **68** 054415
[11] Piekarz P, Parlinski K and Oleś A M 2007 *Phys. Rev.* B **76** 165124
[12] Piekarz P, Parlinski K and Oleś A M 2006 *Phys. Rev. Lett.* **97** 156402
[13] Rowan A D, Patterson C H and Gasparov L V 2009 *Phys. Rev.* B **79** 205103
[14] Ishikawa A, Nohara J and Sugai S 2004 *Phys. Rev. Lett.* **93** 136401
[15] Takubo K, Kubota R, Suzuki T, Kanzaki T, Miyahara S, Furukawa N and Katsufuji T 2011 *Phys. Rev.* B **84** 094406
[16] Reisinger D, Blass B, Klein J, Philipp J B, Schonecke M, Erb A, Alff L and Gross R 2003 *Appl. Phys.* A **77** 619
[17] Honig J M 1995 *J. Alloys Compounds* **229** 24
[18] Shebanova O N and Lazor P 2003 *J. Raman Spectrosc.* **34** 845
[19] Lübbe M, Gigler A M, Stark R W and Moritz W 2010 *Surf. Sci.* **604** 679
[20] Gasparov L V, Choi K-Y, Güntherodt G, Berger H and Forro L 2007 *J. Appl. Phys.* **101** 09G108
[21] Gupta R, Sood A K, Metcalf P and Honig J M 2002 *Phys. Rev.* B **65** 104430
[22] Phase D M, Tiwari S, Prakash R, Dubey A, Sathe V G and Choudhary R J 2006 *J. Appl. Phys.* **100** 123703
[23] Verble J L 1974 *Phys. Rev.* B **9** 5236
[24] Senn M S, Wright J P and Attfield J P 2012 *Nature* **481** 173
[25] Dediu V, Ferdeghini C, Matacotta F C, Nozar P and Ruani G 2000 *Phys. Rev. Lett.* **84** 4489
[26] Schmidt K P, Knetter C, Grüninger M and Uhrig G S 2003 *Phys. Rev. Lett.* **90** 167201
[27] Miyasaka S, Fujioka J, Iwama M, Okimoto Y and Tokura Y 2006 *Phys. Rev.* B **73** 224436
[28] McQueeney R J, Yethiraj M, Montfrooij W, Gardner J S, Metcalf P and Honig J M 2006 *Phys. Rev.* B **73** 174409
[29] Gasparov L V, Rush A, Güntherodt G and Berger H 2009 *Phys. Rev.* B **79** 144303
[30] Bhadram V S, Rajeswaran B, Sundaresan A and Narayana C 2013 *Europhys. Lett.* **101** 17008
[31] Hoesch M, Piekarz P, Bosak A, Le Tacon M, Krisch M, Kozłowski A, Oleś A M and Parlinski K 2013 *Phys. Rev. Lett.* **110** 207204
[32] Bimbi M, Allodi G, De Renzi R, Mazzoli C and Berger H 2008 *Phys. Rev.* B **77** 045115